

# Effects of Multiple Scattering in Cold Nuclear Matter on $J/\psi$ Suppression and $\langle p_T^2 \rangle$ in Heavy Ion Collisions

A.M. Glenn, J.L. Nagle  
University of Colorado at Boulder  
2000 Colorado Avenue  
Boulder, CO 80309, USA

Denes Molnar  
Department of Physics, Purdue University  
525 Northwestern Avenue  
West Lafayette, IN 47907, USA

Coherent multiple scatterings of  $c\bar{c}$  quark pairs in the environment of heavy ion collisions have been used in a previous work by Qiu *et al.* [1] to study  $J/\psi$  suppression. That model suggests that heavy quark re-scatterings in a cold nuclear medium can completely explain the centrality dependence of the observed  $J/\psi$  suppression in  $Pb+Pb$  collisions at the SPS [2]. Their calculations also revealed significant differences under the assumptions of a color singlet or color octet production mechanism. A more recent analytic calculation [3], which includes incoherent final-state re-scatterings with explicit momentum transfer fluctuations in *three* dimensions, indicates much less suppression and little sensitivity to the production mechanism. In this article, we study simultaneously both the  $J/\psi$  suppression and  $p_T$  modifications, at SPS and RHIC energies. We mainly focus on incoherent momentum transfer fluctuations in *two* dimensions, which is more appropriate for the heavy-ion collision kinematics. Our analytic and Monte-Carlo calculations reinforce the analytic results in [3]. Additionally, we find that the experimental  $J/\psi$  suppression and  $\langle p_T^2 \rangle$  from nucleus-nucleus collisions at the SPS or RHIC cannot simultaneously be described in this incoherent multiple scattering framework for any value of the fluctuation strength parameter  $\langle k_T^2 \rangle$ .

PACS numbers: 25.75.-q, 25.75.Nq

## I. INTRODUCTION

Heavy quarkonia ( $c\bar{c}$ ,  $b\bar{b}$ ) have long been of great theoretical and experimental interest as sensitive probes of color deconfinement and thermalization in heavy-ion collisions [4, 5]. The survival probability of these bound states depends on the density and (effective) temperature of the system, leading to the expectation of progressively suppressed quarkonia yields with increasing collision centrality and/or center-of-mass energy.

The most extensively studied quarkonium state is the  $J/\psi$ . The pedagogical picture of  $J/\psi$  formation in nucleus-nucleus collisions proceeds in multiple stages. First, two Lorentz contracted nuclei pass through one another and a particular partonic hard scattering forms a  $c\bar{c}$  pair, a process requiring  $t_{c\bar{c}} \sim \frac{1}{2m_c} \sim 0.01$  fm/c. The pair is then swept through the remaining fast traveling cold nuclear material, of length  $L$ , as shown in Figure 1. This crossing time is up to  $t_{cross} \sim \text{Diameter}_{nucleus}/\gamma \sim 0.1$  fm/c at RHIC (in the center-of-mass frame). A surviving  $c\bar{c}$  pair can form a  $J/\psi$  at  $t_{J/\psi} \sim \text{Radius}_{J/\psi}/c \sim 0.3$  fm/c unless the hot dense medium left in the wake of the nuclear collision, lasting  $t_{medium} \sim 10$  fm/c, interferes. With a suitable model,  $J/\psi$  measurements can therefore help extract, or at least constrain, the properties of the dense medium created in heavy-ion collisions.

A theoretical framework for calculating  $J/\psi$  suppression has been proposed by Qiu, Vary, and Zhang [1]. In their approach (QVZ),  $J/\psi$  production factorizes into two stages: first perturbative production of  $c\bar{c}$  pairs, followed at a much later stage by  $J/\psi$  formation. The corresponding  $A + B \rightarrow J/\psi + X$  production cross section at leading-order in the strong coupling is dependent on the transition probability,  $F(q^2)$  for  $c\bar{c}$  to evolve into a final  $J/\psi$ , where  $q^2$  is the square of the relative momentum of the  $c\bar{c}$  pair. Various  $J/\psi$  formation mechanisms can be accommodated via different  $F$  functions. In QVZ, the  $c\bar{c} \rightarrow J/\psi$  transition probabilities in the color singlet and color octet channels were parameterized as

$$F_{c\bar{c} \rightarrow J/\psi}^{(S)}(q^2) = N_{J/\psi}^{(S)} \theta(q^2) \exp[-q^2/(2\alpha_F^2)] \quad (\text{color singlet}) \quad (1)$$

$$F_{c\bar{c} \rightarrow J/\psi}^{(O)}(q^2) = N_{J/\psi}^{(O)} \theta(q^2) \theta(4m'^2 - 4m_c^2 - q^2) \times \left(1 - \frac{q^2}{4m'^2 - 4m_c^2}\right)^{\alpha_F} \quad (\text{color octet}) \quad (2)$$

where  $m_c$  is the charm quark mass,  $m'$  is the mass scale for the open charm threshold ( $D$  meson mass), and  $N_{J/\psi}$  and  $\alpha_F$  are parameters fixed from hadron-hadron collision data.

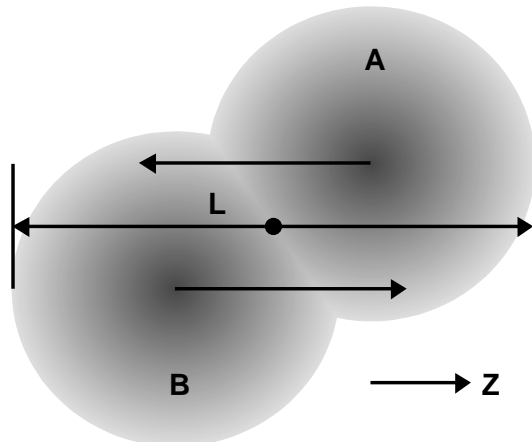


FIG. 1: Diagram of a nucleus-nucleus collision. Arrows at the center of each nucleus indicate the direction of travel. The dot in the center represents a nucleon-nucleon collision, and the distance  $L$  depicts the amount of cold nuclear material a product created in the nucleon-nucleon collision will pass through. The shading of the nuclei indicate the non-uniform density which should be accounted for when calculating  $L$ .

In a nuclear environment, QVZ includes  $J/\psi$  suppression via parton multiple scatterings in cold nuclear matter for the  $c\bar{c}$  pair only, and does not consider further suppression in the hot medium created later. Multiple scattering of the  $c\bar{c}$  pair increases the  $q^2$  of the pair, reducing the overlap with  $F(q^2)$ . The original QVZ modeled this effect with a *constant*  $q^2$  shift linear in nuclear pathlength [1, 6]

$$q^2 \rightarrow q^2 + \Delta q^2 = q^2 + \varepsilon^2 L, \quad (3)$$

which was an intuitive generalization of an identical result for the nuclear broadening in photoproduction of jets given by twist-4 contributions [7]. Surprisingly, this approach was able to reproduce not only hadron-nucleus ( $h+A$ ) but also nucleus-nucleus ( $A+A$ ) data up to SPS energies, including the “anomalous” suppression in  $Pb+Pb$  [2], with the *same*  $\varepsilon^2 \sim 0.2 - 0.3 \text{ GeV}^2/\text{fm}$ . The provocative result indicated negligible additional  $J/\psi$  suppression from the hot medium in energetic heavy-ion collisions, contrary to expected signatures of a dense parton plasma.

A more detailed analysis of coherent multiple scattering effects in the Drell-Yan process [8] also found a constant  $\Delta q^2 \propto L$ , provided one considers at each twist only the contribution that gives the largest  $q^2$  change. The neglected terms, on the other hand, would affect the lower  $\Delta q^2$  region and therefore generate fluctuations in  $\Delta q^2$  at fixed  $L$ . Here we study fluctuations in multiple scatterings of charm quarks and antiquarks in the opposite, *incoherent* scattering limit. In that case, fluctuations in  $\Delta q^2$  are of the same order of magnitude as the average  $\Delta q^2$  for the  $c\bar{c}$  pair. An earlier study[3], which considered momentum transfers in three dimensions, found that fluctuations in  $\Delta q^2$  lead to much weaker suppression in  $A+A$  than in the QVZ approach. While such multiple scatterings of the heavy quarks are expected to have a direct impact on the  $J/\psi$   $p_T$  distributions [9, 10], the QVZ and Fujii [3] calculations do not provide any information about  $p_T$ . In this work we focus on the interplay between the  $J/\psi$  yield and  $\langle p_T^2 \rangle$  based on a Monte-Carlo approach.

## II. ROLE OF MOMENTUM TRANSFER FLUCTUATIONS

In the QVZ framework, final-state quark scatterings affect the momentum distribution of  $c\bar{c}$  pairs and therefore the  $J/\psi$  yield as

$$dN_{J/\psi} = F(q^2) \int d\Delta q^2 P(\Delta q^2; q^2 - \Delta q^2) dN_{c\bar{c}}(q^2 - \Delta q^2) \equiv F(q^2) d\bar{N}_{c\bar{c}}(q^2), \quad (4)$$

where  $P(\Delta q^2; q^2)$  is the probability of accumulating a total  $\Delta q^2$  change in the relative pair momentum given an initial value  $q^2$ . A completely equivalent approach is to group scattering effects into a modified formation probability  $\bar{F}$

$$dN_{J/\psi} = dN_{c\bar{c}}(q^2) \int d\Delta q^2 P(\Delta q^2; q^2) F(q^2 + \Delta q^2) \equiv \bar{F}(q^2) dN_{c\bar{c}}(q^2), \quad (5)$$

which has the advantage that the primary  $c\bar{c}$  distribution and final state effects factorize.

The effective formation probability can be calculated from a model of final state interactions in the medium. We consider here incoherent Gaussian momentum kicks in *two* dimensions transverse to the beam axis, independently for each quark (i.e., ignore correlations between  $c$  and  $\bar{c}$ ), as a model of small-angle scatterings off fast partons. This results in momentum-space random walk probability distributions

$$g(\vec{k}_{T,i}) = \frac{2}{\pi L \varepsilon^2} \exp\left[-\frac{2\vec{k}_{T,i}^2}{L \varepsilon^2}\right] \quad (i = 1, 2 \text{ for } c, \bar{c}), \quad (6)$$

where  $\vec{k}_{T,i}$  is the total momentum transferred, while  $\varepsilon^2/2$  is average momentum-squared transferred per unit nuclear pathlength. The average momentum and the average relative momentum transferred to the  $c\bar{c}$  pair,  $\vec{k}_T \equiv \vec{k}_{T,1} + \vec{k}_{T,2}$  and  $\Delta\vec{k}_T \equiv \vec{k}_{T,1} - \vec{k}_{T,2}$ , are also Gaussian but with dispersions  $L \varepsilon^2$ .

In the nonrelativistic limit, the accumulated change in the relative pair momentum is

$$\Delta q^2 \approx \Delta \vec{q}^2 = (\vec{q} + \vec{k}_T)^2 - \vec{q}^2 = \Delta k_T^2 + 2\Delta k_T q \cos \theta. \quad (7)$$

Final state scatterings can be considered at three levels of sophistication:

- i) constant shift (CS)* - keep only the *average* of the first term, i.e.,  $\Delta q^2 \rightarrow L \varepsilon^2$  as in (3);
- ii) partial fluctuations (PF)* - keep fluctuations in the magnitude  $\Delta k_T^2$  but ignore the second angular term, i.e.,  $\Delta q^2 \rightarrow \Delta k_T^2$ ; and
- iii) all fluctuations (ALL)* - keep fluctuations both in magnitude and direction, i.e., the full expression (7).

In the color singlet case, the effective transition probabilities are calculable analytically in a straightforward manner:

$$\begin{aligned} \bar{F}_{CS}^{(S)}(q^2) &= N_{J/\psi}^{(S)} \exp\left[-\frac{q^2 + L \varepsilon^2}{2\alpha_F^2}\right] \\ \bar{F}_{PF}^{(S)}(q^2) &= N_{J/\psi}^{(S)} \frac{2\alpha_F^2}{2\alpha_F^2 + L \varepsilon^2} \exp\left[-\frac{q^2}{2\alpha_F^2}\right] \\ \bar{F}_{ALL,2D}^{(S)}(q^2) &= N_{J/\psi}^{(S)} \frac{2\alpha_F^2}{2\alpha_F^2 + L \varepsilon^2} \exp\left[-\frac{\vec{q}_T^2}{2\alpha_F^2 + L \varepsilon^2} - \frac{Q_0^2}{2\alpha_F^2}\right] \\ &= N_{J/\psi}^{(S)} \frac{2\alpha_F^2}{2\alpha_F^2 + L \varepsilon^2} \exp\left[-\frac{q^2}{2\alpha_F^2 + L \varepsilon^2}\right] \exp\left[-\frac{L \varepsilon^2 Q_0^2}{2\alpha_F^2(2\alpha_F^2 + L \varepsilon^2)}\right] \\ \bar{F}_{ALL,3D}^{(S)}(q^2) &= N_{J/\psi}^{(S)} \left(\frac{3\alpha_F^2}{3\alpha_F^2 + L \varepsilon^2}\right)^{3/2} \exp\left[-\frac{3\vec{q}^2}{6\alpha_F^2 + 2L \varepsilon^2} + \frac{q_0^2}{2\alpha_F^2}\right] \\ &= N_{J/\psi}^{(S)} \left(\frac{3\alpha_F^2}{3\alpha_F^2 + L \varepsilon^2}\right)^{3/2} \exp\left[-\frac{3q^2}{6\alpha_F^2 + 2L \varepsilon^2}\right] \exp\left[\frac{L \varepsilon^2 q_0^2}{2\alpha_F^2(3\alpha_F^2 + L \varepsilon^2)}\right], \end{aligned} \quad (8)$$

where  $Q_0^2 \equiv q_z^2 - q_0^2$ ,  $q^2 \equiv \vec{q}_T^2 + Q_0^2$ , and the last two lines are for Gaussian scattering in three dimensions. If fluctuations are neglected,  $\bar{F}$  is strongly suppressed, exponentially with pathlength. This results in exponential  $J/\psi$  suppression with a suppression factor  $R_{J/\psi} = \exp[-L \varepsilon^2/(2\alpha_F^2)]$ . Fluctuations in the magnitude of  $\Delta\vec{k}_T$  change the behavior to a milder power-law reduction with  $L$ ,  $R_{J/\psi} = 2\alpha_F^2/(2\alpha_F^2 + L \varepsilon^2)$ . The biggest effect, however, comes from fluctuations in the direction of  $\Delta\vec{k}_T$ . These broaden  $\bar{F}$  compared to the original  $F(q^2)$ , further weakening suppression effects. It is easy to understand why angle fluctuations are important. From any starting point in momentum space, there is always a finite probability for the random walk to get *closer* to the origin, thereby enhancing the formation probability compared to the other two approximations where any initial  $q^2$  can only grow.

Figure 2 illustrates the influence of fluctuations and confirms the above general considerations. The left plot shows the color singlet  $\bar{F}(q^2)$  resulting from the different fluctuation treatments, for the original QVZ parameter set  $N_{J/\psi} = 0.47$ ,  $\alpha_F = 1.15$ , and with  $\varepsilon^2 = 0.3 \text{ GeV}^2/\text{fm}$  and a pathlength  $L = 8 \text{ fm}$  characteristic of near-central  $Pb+Pb$  or  $Au+Au$  collisions. The right plot shows the corresponding  $J/\psi$  suppression factors (relative to the  $L = 0$  case) as a function of  $L \varepsilon^2$ , for an initial  $c\bar{c}$  distribution in  $p+p$  events at  $\sqrt{s} = 200 \text{ GeV}$  from the PYTHIA [11] event generator program (the PYTHIA results can be parameterized as  $dN_{c\bar{c}}/dq^2 \propto (q^2)^{0.518}/[2.08 \cdot 10^6 + (\sqrt{q^2}/(1 \text{ GeV}^2) + 4.04)^{8.15}]$ ). Clearly, the largest suppression comes from the simplest, constant shift approximation (dashed-dotted line). On the other hand, the inclusion of fluctuations gives a much-reduced suppression (solid line). For comparison we also show

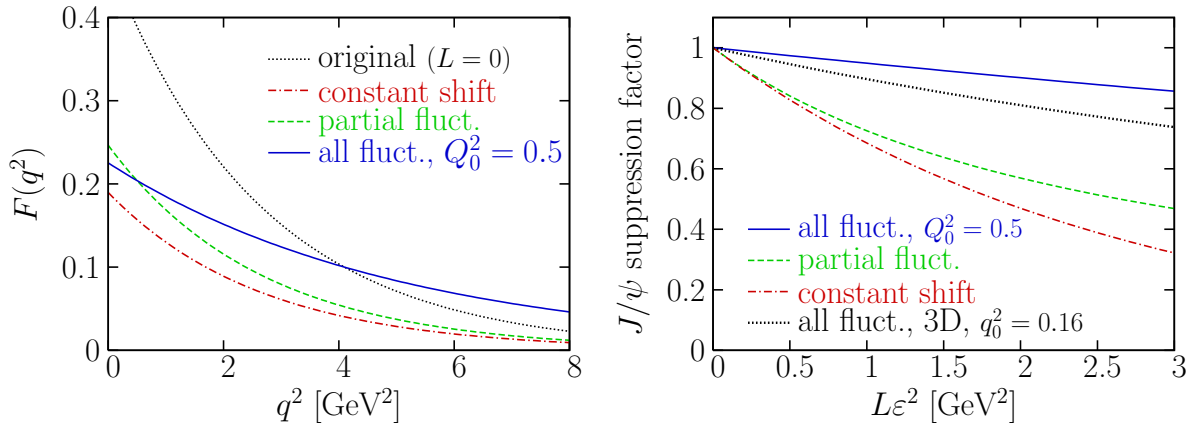


FIG. 2: *Left plot:* effective  $c\bar{c} \rightarrow J/\psi$  transition probability in the color-singlet channel for  $L\epsilon^2 = 8 \times 0.3$  GeV<sup>2</sup> (characteristic of near-central  $Pb + Pb$  or  $Au + Au$  collisions) with three different approaches to treat fluctuations in final-state interactions. Results for the constant shift (dashed-dotted) and “partial fluctuation” (dashed) approximations (see text) are compared to the full 2D Gaussian random walk result, assuming  $Q_0^2 = 0.5$  GeV<sup>2</sup>, (solid) and the case of no final-state interactions (dotted). The full result is much broader in  $q^2$ , resulting in much weaker  $J/\psi$  suppression. *Right plot:* suppression of the total  $J/\psi$  in nuclear collisions at  $\sqrt{s_{NN}} = 200$  GeV as a function of  $L\epsilon^2$  for the constant shift (dashed-dotted), partial fluctuation (dashed) approximations, and the full 2D Gaussian random walk result (solid). The full result gives much smaller suppression than the two approximations. Results for the 3D random walk in [3] are also shown (dotted), for  $q_0^2 = 0.16$  GeV<sup>2</sup>.

the result for the *three-dimensional* Gaussian random walk considered in [3] (dotted line), which gives a stronger suppression than the more realistic 2D case. The reason is that in 3D, angle fluctuations have a weaker role because the solid angle  $\sin\theta d\theta d\phi$  prefers  $\theta$  values near  $\pi/2$ , for which the angular term in (7) is small. Though in the very-large- $L$  limit the suppression factor behaves as  $1/L$  and  $1/L^{3/2}$  for 2D and 3D random walk respectively [3], we found that in practice these limits apply poorly and give more suppression at moderate  $L\epsilon^2 \sim 0.5 - 5$  GeV<sup>2</sup> than even the constant shift approximation. All the above trends apply to the color octet case as well.

We note that in the simple analytic calculation above we applied (8) with a constant  $Q_0^2 = 0.5$  GeV<sup>2</sup> (2D case) and  $q_0^2 = 0.16$  GeV<sup>2</sup> (3D case), which are the average values for midrapidity  $J/\psi$ -s coming from the region  $q^2 \sim 0 - 3$  GeV<sup>2</sup> that gives the dominant contribution to the yield [12]. In general, the various  $q$  components are correlated (e.g.,  $Q_0^2 \leq q^2$ ) and therefore the calculation would require  $dN/dq^2 dQ_0^2$  (2D) or  $dN/dq^2 dq_0^2$  (3D) in analytic form as an input. We include the  $q^2 - Q_0^2$  correlations for 2D random walk in Sec. III using a Monte-Carlo approach.

If the strength of momentum kicks per unit pathlength  $\epsilon^2$  were an unknown parameter, much of the above discussion would be academic because we found that in the calculation above each approximation can reproduce the exact result quite well with an appropriate rescaling of  $\epsilon^2$ . In particular,  $\epsilon_{CS}^2 : \epsilon_{PF}^2 : \epsilon_{ALL,2D}^2 : \epsilon_{ALL,3D}^2 \approx 1 : 1.5 : 9.5 : 5$  [13]. However, an independent determination of  $\epsilon^2$  from FermiLab data on dijet momentum imbalance already constrains  $\epsilon^2$  to  $\sim 0.2 - 0.5$  GeV<sup>2</sup>/fm [7].

Even if  $\epsilon^2$  were arbitrary, it affects not only the  $J/\psi$  yields but also the spectra. In particular the larger the  $\epsilon^2$ , the higher the  $\langle p_T^2 \rangle$  of the  $J/\psi$ 's. In the following sections we analyze the suppression- $\langle p_T^2 \rangle$  consistency in detail and contrast it to data from the SPS and RHIC, using a Monte-Carlo approach. For the spectra, both initial and final state scatterings are important.

### III. MONTE-CARLO STUDY

In this study we utilize a Monte-Carlo Glauber model [14] calculation, as implemented in the Heavy Ion community [15, 16], which assumes a 30 mb and 42 mb nucleon-nucleon cross section for  $\sqrt{s_{NN}} = 17.2$  and 200 GeV respectively, for collision geometry. We consider a nucleus-nucleus collision at a given impact parameter and collision energy, and for each binary collision assign a  $c\bar{c}$  pair with momentum vectors from charm events in  $p+p$  collisions (at the same  $\sqrt{s_{NN}}$ ) from PYTHIA 6.205 with the parameters used in Section II [11]. The pathlength depicted in Fig. 1,  $L \equiv L_A + L_B$ , is the sum of contributions by nucleons moving towards the production point from the left and right, which are calculated by integrating over the nuclear density distribution and dividing by the density at the center of

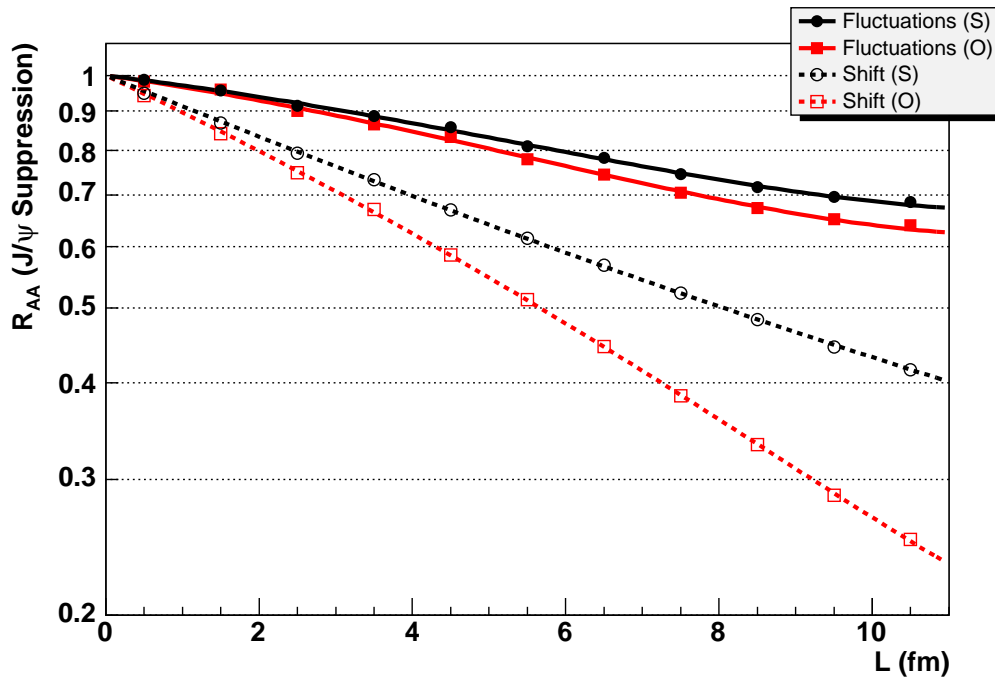


FIG. 3: The dependence of  $J/\psi$  suppression on collision centrality for  $\sqrt{s_{NN}} = 17.2$  GeV  $Pb+Pb$  collisions for  $\langle k_T^2 \rangle = 0.3$  GeV $^2$ . The filled markers indicate results from the model with  $q^2$  changes due to re-scattering including fluctuations. The open markers show results when the explicit re-scattering is replaced by an overall shift which results in the same average  $q^2$  increase per unit pathlength,  $\Delta q^2/L \equiv \varepsilon^2 = 0.27$  GeV $^2$ /fm. “S”(circles) and “O”(squares) refer to the color singlet and color octet transition probabilities (see Eqs. (1) and (2)).

the nucleus. E.g., for a production point  $(\vec{x}_T, z_0)$  relative to the center of nucleus A

$$L_A(\vec{x}_T, z_0) \equiv \frac{1}{\rho_{max}} \int_{z_0}^{\infty} dz \rho(\sqrt{z^2 + \vec{x}_T^2}) = \frac{\langle N_{coll}(\vec{x}_T, z_0) \rangle}{\rho_{max} \sigma_{inel}^{N+N}}, \quad (9)$$

where  $\langle N_{coll} \rangle$  is the average number of remaining binary collisions on the right and  $\sigma_{inel}^{N+N}$  is the inelastic nucleon-nucleon cross section. Final state scatterings are modeled via a 2D Gaussian random walk as described in Section II except that, instead of the continuous  $L\varepsilon^2$  variable, the number of scatterings is quantized in terms of the binary collisions, where the average momentum transfer squared per scattering is  $\langle k_T^2 \rangle$ ; i.e., in the Monte-Carlo  $N_{coll}\langle k_T^2 \rangle$  is equivalent to  $L\varepsilon^2$  in the analytic calculations. We confirmed via increasing the kicks per binary collision, while reducing the  $\langle k_T^2 \rangle$  by the same factor, that the discretization does not have a significant effect on our results. For initial state scatterings, which are meant to represent the scattering of individual incoming partons (mainly gluons) before the  $c\bar{c}$  production, the  $k_T$  is transferred to the  $p_T$  of the  $c\bar{c}$  pair with no increase in the  $q^2$ . For simplicity, we assume that the  $\langle k_T^2 \rangle$  for initial state parton scatterings is the same as for the final state parton scatterings.

From Eq. (9) it is clear that the  $\langle k_T^2 \rangle$  parameter in the Monte-Carlo is proportional to  $\varepsilon^2$ , the average increase in  $q^2$  per unit nuclear pathlength. The constant of proportionality depends on the collision energy (through the inelastic nucleon-nucleon cross section) and also the nuclear density at the center of the colliding nuclei. For convenience, we tabulate in Table I several  $\langle k_T^2 \rangle$  values and the corresponding  $\varepsilon^2$ , for  $Pb + Pb$  collisions at  $\sqrt{s_{NN}} = 17.2$  GeV (top SPS energy).

As a consistency check, instead of our multiple scattering model, we study  $J/\psi$  suppression as a function of  $L$  for  $\sqrt{s_{NN}} = 17.2$  GeV  $Pb+Pb$  collisions via the  $q^2 = q^2 + \varepsilon^2 L$  shift as done by QVZ. The only difference is that we use the PYTHIA  $q^2$  distribution for  $c\bar{c}$  pairs. The results, shown in Fig. 3 and labeled ‘Shift’, give similar suppression trends to those reported in [1]. In particular, we observe the larger suppression as a function of  $L$  for the color octet transition probability  $F^{(O)}(q^2)$  (defined in Eq. (2)). For the Monte-Carlo studies, we use  $N_{J/\psi} = 0.47$  and  $\alpha_F = 1.2$  for  $F^{(S)}(q^2)$  and  $N_{J/\psi} = 0.485$  and  $\alpha_F = 1$  for  $F^{(O)}(q^2)$  (consistent with Sec. II and QVZ [1]).

Figure 3 also shows a comparison of  $J/\psi$  suppression in the shifted  $q^2$  model and the fluctuation model. Just like for the analytic study in Section II, we keep the average  $q^2$  shift the same in both cases and therefore use  $\langle k_T^2 \rangle = 0.3$

TABLE I: The  $\varepsilon^2 \equiv \Delta\langle q^2 \rangle/L$  values corresponding to various  $\langle k_T^2 \rangle$  parameter values for  $\sqrt{s_{NN}} = 17.2$  GeV  $Pb + Pb$  collisions.

$\langle k_T^2 \rangle$ (GeV <sup>2</sup> )	$\varepsilon^2 \equiv \Delta\langle q^2 \rangle/L$ (GeV <sup>2</sup> /fm)
0.1	0.09
0.2	0.18
0.3	0.27
0.4	0.36

TABLE II: Results for  $J/\psi$  properties from the model for minimum bias collisions in  $\sqrt{s_{NN}} = 200$  GeV  $d+Au$  for several values of input  $\langle k_T^2 \rangle$ .

$\langle k_T^2 \rangle$ (GeV <sup>2</sup> )	Suppression ( $R_{dAu}$ )	$\Delta\langle p_T^2 \rangle$ (GeV <sup>2</sup> )
0.0	1.00	0.0
0.075	0.95	0.6
0.15	0.91	1.3
0.225	0.87	1.8
0.3	0.84	2.4

GeV<sup>2</sup> in the Monte Carlo, which corresponds to  $\varepsilon^2 = 0.27$  GeV<sup>2</sup>/fm, a shift consistent with range used by QVZ in [1]. We find that fluctuations give significantly less suppression. Clearly, an incoherent random walk type process cannot be consistent with the  $\bar{q}^2 = q^2 + \varepsilon^2 L$  shift since the most probable scattering value is zero and the low  $q^2$  region therefore cannot be completely depleted. We note that our numerical results agree with the analytic ones presented for the singlet case in Section II.

In addition, the suppression patterns for the color singlet and color octet transition probabilities,  $F^{(S)}(q^2)$  and  $F^{(O)}(q^2)$ , become nearly indistinguishable when fluctuations are included. Therefore, we only report results for the octet case for the remainder of this study. This is in agreement with the previous analytic calculations [3] that incorporated momentum transfer fluctuations in three dimensions.

#### IV. RESULTS

We first use the model to study suppression and  $p_T$  distributions in  $p(d)+Au$  collisions at SPS and RHIC energies. High statistics data are available for comparison from the NA50 experiment. In Figure 4 we show results for  $\langle k_T^2 \rangle$  values which reasonably reproduce either the  $\Delta\langle p_T^2 \rangle = \langle p_T^2 \rangle_{p+A} - \langle p_T^2 \rangle_{p+p}$  or the suppression as a function of the nuclear path-length. For  $p+A$ , a  $\langle k_T^2 \rangle = 0.3$  GeV<sup>2</sup> reproduces the  $R_{pA}$  dependence, but produces far too much  $\Delta\langle p_T^2 \rangle$  increase. A  $\langle k_T^2 \rangle = 0.05$  GeV<sup>2</sup>, which is consistent with the  $\Delta\langle p_T^2 \rangle$  trend, under predicts the suppression for the largest nuclei. Even for  $p+A$  the model cannot simultaneously give satisfactory descriptions of  $\Delta\langle p_T^2 \rangle$  and  $R_{pA}$  for any  $\langle k_T^2 \rangle$  for large nuclei. We note that the relative strength of initial and final state scatterings is not tuned in our model, but since the initial state scatterings currently account for roughly half of the  $\Delta\langle p_T^2 \rangle$  increase, removing initial state scatterings would not be sufficient to bring the model into good agreement with the data. Calculations for  $\sqrt{s_{NN}} = 200$  GeV  $d+Au$  using the same  $\langle k_T^2 \rangle$  values are also shown in Figure 4.

Experimental measurements of  $J/\psi$  suppression  $R_{dAu}$  and  $\Delta\langle p_T^2 \rangle$  have recently been made by the PHENIX collaboration at RHIC [17]. They report  $\langle p_T^2 \rangle_{d+Au} - \langle p_T^2 \rangle_{p+p} = 1.77 \pm 0.37, 1.12 \pm 0.33, \text{ and } -1.28 \pm 0.94$  and  $R_{dAu} = 1.18 \pm 0.12, 0.79 \pm 0.06, \text{ and } 0.95 \pm 0.1$  for backward, forward, and mid rapidity respectively in minimum bias deuteron-gold reactions. Table II shows our Monte-Carlo results for various  $\langle k_T^2 \rangle$  values. Although no strong statement of consistency can be made due to current experimental errors, the results from our model for  $\langle k_T^2 \rangle > 0.3$  GeV<sup>2</sup> can be safely excluded from simultaneously satisfying both experimental  $R_{dAu}$  and  $\Delta\langle p_T^2 \rangle$  constraints. We note that this level of suppression is consistent with that determined from a simple nuclear absorption Glauber model with a cross section  $\sigma_{J/\psi-N} \approx 1 - 3$  mb [18], which we have also confirmed. Future measurements of  $J/\psi$  in deuteron or proton-nucleus reactions with sufficient statistics for centrality dependencies to be accurately determined will be important to narrow this parameter range.

Despite the inability of this model to fully describe the  $p(d)+Au$  data, we feel it is useful to follow through with

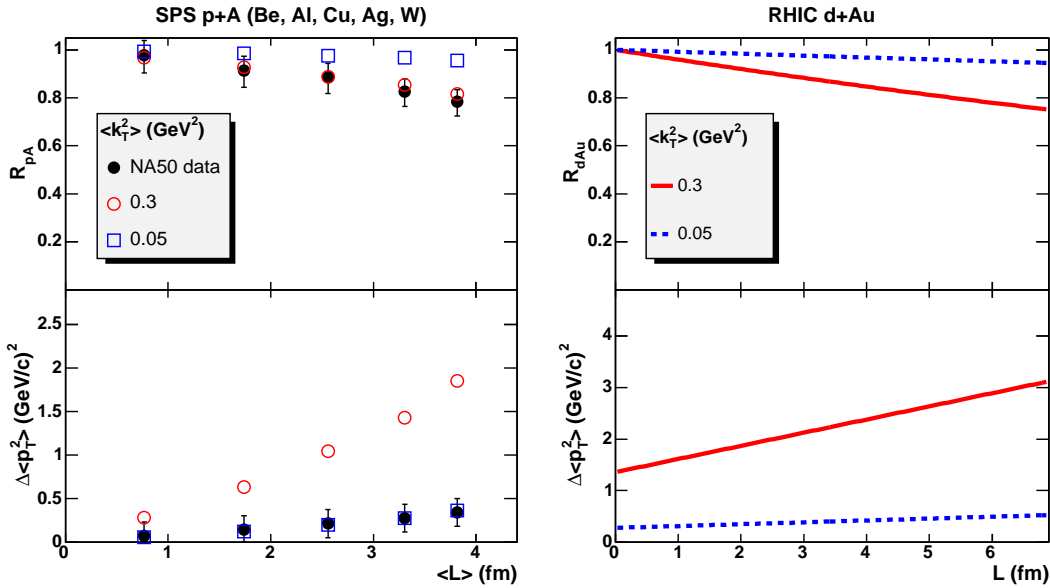


FIG. 4: *Left plots:* The nuclear modification factor (Upper) and  $\Delta \langle p_T^2 \rangle$  (Lower) for  $J/\psi$  for 400 GeV/c proton beams incident on several fixed targets as a function of the mean nuclear path-length  $\langle L \rangle$ . The filled circles show data from NA50 measurements [21]. The suppression data uses the  $p+p$  value scaled from 450 GeV/c, and the  $p+p$  reference value for  $\langle p_T^2 \rangle$  of  $1.6 \text{ (GeV/c)}^2 \pm 10\%$  comes from the projection of a fit to the  $\langle p_T^2 \rangle$   $p+A$  data to  $L = 0$  fm. The errors for both graphs are dominated by the  $p+p$  reference, so they are highly correlated. *Right plots:* calculations for  $\sqrt{s_{NN}} = 200$  GeV  $d+Au$  collisions. Note that for the left plots each  $\langle L \rangle$  comes from a different target nucleus, while for the right plots the  $L$  is for different production point geometries. The calculations use the  $F^{(O)}(q^2)$  transition probability.

heavy ion results. For a high-temperature quark-gluon plasma, the incoherent final-state scattering assumption is more justified because the Debye length is much smaller than the mean free path  $\mu_D^{-1} \sim (gT)^{-1} \ll \lambda \sim (g^2T)^{-1}$  [19]. Here we report results for  $Pb+Pb$  collisions at  $\sqrt{s_{NN}} = 17.2$  GeV. Figure 5 shows the  $J/\psi$  suppression relative to binary collision scaling  $R_{AA}$  and  $\Delta \langle p_T^2 \rangle$  as a function of centrality for various  $\langle k_T^2 \rangle$  values. As  $\langle k_T^2 \rangle$  is increased, the fraction of surviving  $J/\psi$  decreases and the  $\langle p_T^2 \rangle$  of the surviving  $J/\psi$  increases. Figure 5 also shows data points from the NA50 experiment [2, 20]. The general suppression trend is not well reproduced by any value of  $\langle k_T^2 \rangle$ . A value of  $\langle k_T^2 \rangle$  which reproduces the suppression for the most central events substantially over-predicts the increase in  $\langle p_T^2 \rangle$ . The effect of heavy quark re-scattering in a cold nuclear medium, as described in this model, cannot explain the NA50 data.

Lastly, we use the model to study suppression and  $p_T$  distributions in  $Au+Au$  collisions at  $\sqrt{s_{NN}} = 200$  GeV. The  $R_{AA}$  and  $\Delta \langle p_T^2 \rangle$  results are shown for  $Au+Au$  in Fig. 6, which again demonstrates the strong correlation between increased suppression, from  $q^2$  change, and increased  $\Delta \langle p_T^2 \rangle$  in models using this type of multiple scatterings of  $c$  and  $\bar{c}$  quarks to account for  $J/\psi$  suppression. For  $\langle k_T^2 \rangle = 0.3$  GeV<sup>2</sup>, roughly the largest value consistent with  $d+Au$  data, the fairly weak suppression,  $R_{AA} \sim 0.7$ , requires  $\Delta \langle p_T^2 \rangle \sim 5$  GeV<sup>2</sup>.

We highlight this connectedness and the inconsistency with available RHIC and SPS data for central events in Fig. 7. We show that for any parameter values of  $\langle k_T^2 \rangle$  one is constrained to be on a curve correlating suppression and  $p_T$ . The SPS data are far from the  $R_{AA}$  vs  $\Delta \langle p_T^2 \rangle$  curve. We note that preliminary data from the PHENIX experiment also appear to be inconsistent with any points on the curve [22]. For a given  $\langle p_T^2 \rangle$ , the suppression at the SPS is stronger because for a lower collision energy the initial  $c\bar{c}$   $q^2$  distribution is narrower, and therefore the yield is more sensitive to rescattering (i.e., shifts in  $q^2$ ). Although this study does not account for nuclear modifications of the parton distribution function (i.e., effects such as nuclear shadowing), these effects do not appear significant enough to change the basic conclusions of our study [18, 23].

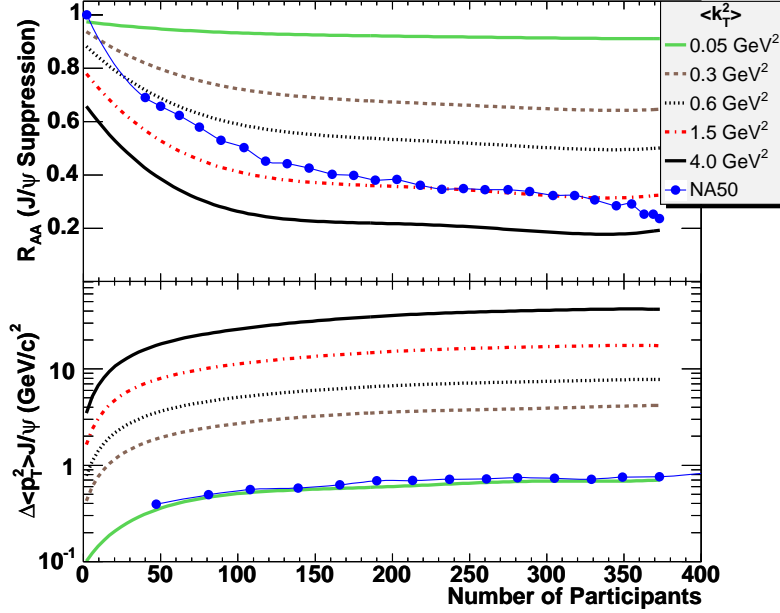


FIG. 5: The nuclear modification factor and  $\Delta\langle p_T^2 \rangle$  for  $J/\psi$  in  $\sqrt{s_{NN}} = 17.2$  GeV  $Pb+Pb$  collisions as a function of the number of participants for several input values of  $\langle k_T^2 \rangle$ . The filled circles show data from NA50 measurements [2, 20]. The calculations use the  $F^{(O)}(q^2)$  transition probability.

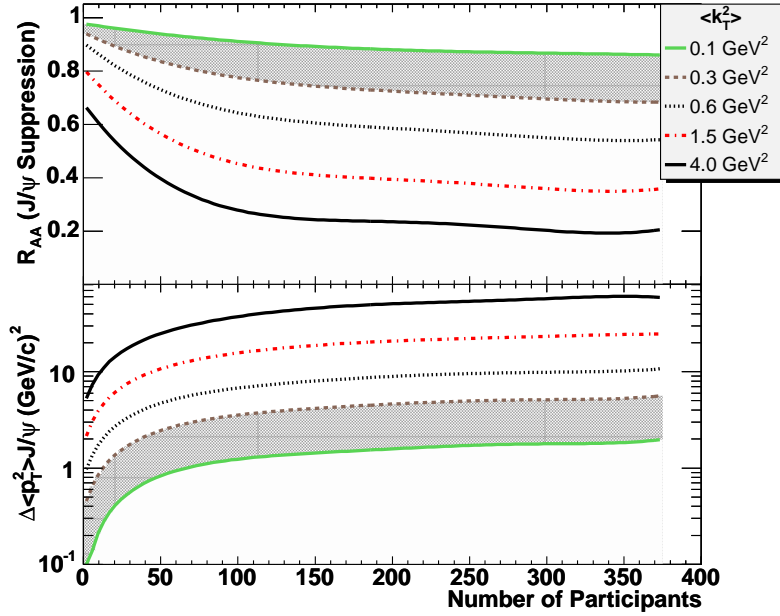


FIG. 6: The nuclear modification factor and  $\Delta\langle p_T^2 \rangle$  for  $J/\psi$  in  $\sqrt{s_{NN}} = 200$  GeV  $Au+Au$  collisions as a function of the number of participants for several input values of  $\langle k_T^2 \rangle$ . The shaded area represents the range of  $\langle k_T^2 \rangle$  values which are in rough agreement with the PHENIX  $d+Au$  data [17]. Our calculations use the color octet  $F^{(O)}(q^2)$  transition probability.

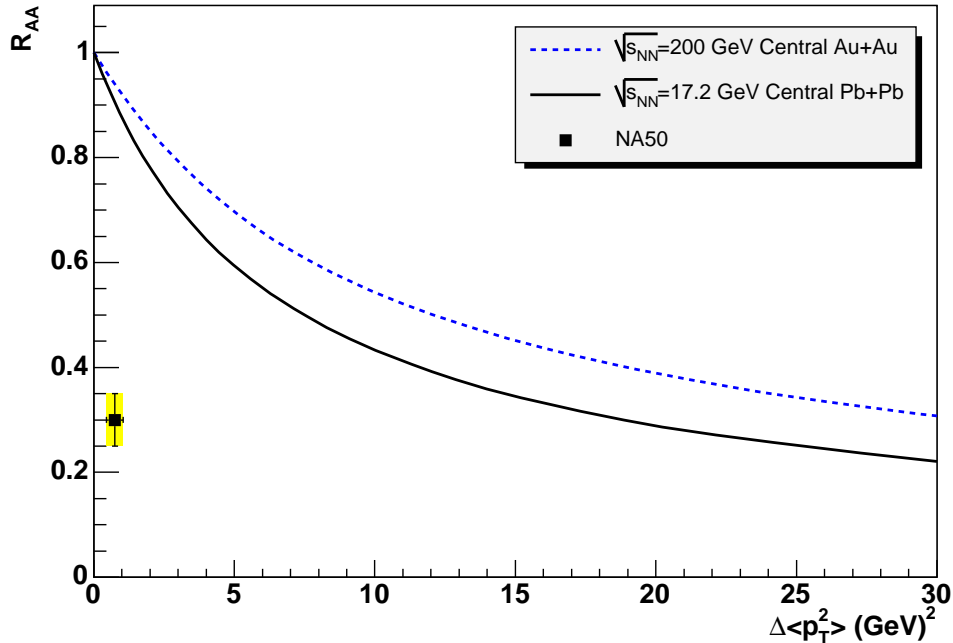


FIG. 7: The  $R_{AA}$  vs  $\Delta\langle p_T^2 \rangle$  curves traced by varying  $\langle k_T^2 \rangle$  for events with 300-350 participants (central) for  $Au+Au$  and  $Pb+Pb$  collisions at RHIC and SPS energies respectively. The black square shows the value from NA50 measurements [2, 20].

## V. CONCLUSIONS

We have presented a Monte-Carlo model for calculating the effect of initial and final state re-scattering in cold nuclear matter on the production and suppression of  $J/\psi$  in heavy ion collisions. Although largely motivated by an earlier work from Qiu, Vary, and Zhang (QVZ) [1], we obtain significantly different results at a given rescattering "strength"  $\langle k_T^2 \rangle$  due to the use of *incoherent* scatterings, which give considerable fluctuations in the change of relative  $c\bar{c}$  pair momentum as opposed to the overall shift expected intuitively based on coherent re-scattering studies of jet photoproduction and Drell-Yan[6, 7, 8]. Similar observations were previously discussed by Fujii [3] based on a three-dimensional Gaussian random walk model. Our analytic and numerical results indicate that, for a more realistic 2D random walk, momentum transfer fluctuations have an even stronger effect. These results highlight the importance of calculating the  $q^2$  modification for a  $c\bar{c}$  pair undergoing coherent multiple scattering in cold nuclear matter, including the first nonvanishing contribution to fluctuations in  $\Delta q^2$ [8].

In addition, we demonstrate a direct correlation between  $\Delta\langle p_T^2 \rangle \equiv \langle p_T^2 \rangle_{A+A} - \langle p_T^2 \rangle_{p+p}$  and the  $J/\psi$  suppression factor  $R_{AA}$  in the incoherent multiple scattering model. We explore  $J/\psi$  suppression and  $\Delta\langle p_T^2 \rangle$  in  $\sqrt{s_{NN}} = 17.2$  GeV  $Pb+Pb$  and  $\sqrt{s_{NN}} = 200$  GeV  $Au+Au$  collisions as a function of centrality for a wide range of  $\langle k_T^2 \rangle$  parameter values, and find that it impossible for this class of models to *simultaneously* satisfy both suppression and  $\langle p_T^2 \rangle$  constraints from available nucleus-nucleus data at SPS or RHIC. It would be interesting to compare these results with the suppression -  $\langle p_T^2 \rangle$  correlation given by coherent multiple scatterings.

The importance of heavy quarkonia is emphasized by recent puzzling observations regarding open heavy flavor in  $Au+Au$  reactions at RHIC. Spectra [24, 25] and azimuthal anisotropy  $v_2(p_T) \equiv \langle \cos 2\phi \rangle_{p_T}$  [26] of "non-photonic" single electrons indicate a striking modification of heavy quark momentum distributions in medium. We are extending our Monte-Carlo calculation for  $J/\psi$  by incorporating these  $c\bar{c}$  pairs into the parton cascade model [27] to thus include not only cold nuclear matter effects, but those of the hot medium as well. Finally, we note that our framework could also be applied to study nuclear effects on other heavy-flavor mesons, such as  $b\bar{b}$  states, and open charm and bottom.

## VI. ACKNOWLEDGMENTS

We acknowledge a careful reading of the manuscript by David Silvermyr.

This work is supported by the Director, Office of Science, Office of High Energy and Nuclear Physics, Division of Nuclear Physics, of the U.S. Department of Energy under Grant No. DE-FG02-00ER41152 (AMG and JLN). DM thanks RIKEN, Brookhaven National Laboratory and the US Department of Energy [DE-AC02-98CH10886] for providing facilities essential for the completion of this work.

- 
- [1] J. Qiu, J. P. Vary and X. Zhang, Phys. Rev. Lett. **88**, 232301 (2002).  
 J. w. Qiu, J. P. Vary and X. f. Zhang, Nucl. Phys. A **698**, 571 (2002) [arXiv:nucl-th/0106040].
- [2] M. C. Abreu *et al.* [NA50 Collaboration], Phys. Lett. B **521**, 195 (2001).
- [3] H. Fujii, Phys. Rev. C **67**, 031901 (2003).
- [4] T. Matsui and H. Satz, Phys. Lett. B **178**, 416 (1986).
- [5] R. L. Thews and M. L. Mangano, arXiv:nucl-th/0505055.
- [6] C.J. Benesh, J. Qiu, J. P. Vary, Phys. Rev. C **50**, 1015 (1994).
- [7] M. Luo, J. w. Qiu and G. Sterman, Phys. Rev. D **49**, 4493 (1994).
- [8] R. J. Fries, Phys. Rev. D **68**, 074013 (2003).
- [9] D. Kharzeev, M. Nardi and H. Satz, Phys. Lett. B **405**, 14 (1997) [arXiv:hep-ph/9702273].
- [10] J. L. Nagle and M. J. Bennett, Phys. Lett. B **465**, 21 (1999) [arXiv:nucl-th/9907004].
- [11] We used PYTHIA 6.154 with CTEQ5M1 parton distribution functions, a  $c$  quark mass of 1.25 GeV  $\text{PMAS(PYCOMP(4, 1))} = 1.25$ ,  $\langle k_T \rangle = 1.5$  GeV  $\text{PARP(91)} = 1.5$ , and a  $k_T$  cutoff of 5.0 GeV  $\text{PARP(93)} = 5.0$ .
- [12] The average  $Q_0^2 = q_z^2 - q_0^2$  is largely independent of the  $J/\psi$  rapidity  $y$ . However, the average  $q_0^2$  grows with  $|y|$ .
- [13] This is roughly consistent with a comparison of results by Qiu *et al.* [1] and Fujii [3]. They use similar numerical values for  $\varepsilon^2$ , however, in [3],  $\varepsilon^2$  is multiplied by an additional factor of 3. We need to scale by a larger factor of 5 because, unlike Fujii, we consider a nonzero  $q_0^2$  (cf. Eq. (8)).
- [14] R. J. Glauber and G. Matthiae, Nucl. Phys. B **21**, 135 (1970).
- [15] B. B. Back *et al.* [PHOBOS Collaboration], Phys. Rev. C **65**, 031901 (2002) [arXiv:nucl-ex/0105011].
- [16] K. Adcox *et al.* [PHENIX Collaboration], Phys. Rev. Lett. **88**, 022301 (2002) [arXiv:nucl-ex/0109003].
- [17] S. S. Adler *et al.*, Phys. Rev. Lett. **96**, 012304 (2006) [arXiv:nucl-ex/0507032].
- [18] R. Vogt, arXiv:nucl-th/0507027.
- [19] This assumption is also made by studies of radiative parton energy loss [28, 29].
- [20] M. C. Abreu *et al.* [NA50 Collaboration], Phys. Lett. B **499**, 85 (2001).
- [21] N. S. Topilskaya *et al.* [NA50 Collaboration], Nucl. Phys. A **715**, 675 (2003);  
 B. Alessandro *et al.* [NA50 Collaboration], Eur. Phys. J. C **33**, 31 (2004).
- [22] H. Pereira Da Costa *et al.* [PHENIX Collaboration], [arXiv:nucl-ex/0510051].
- [23] R. Vogt, Phys. Rev. C **71**, 054902 (2005) [arXiv:hep-ph/0411378].
- [24] S. S. Adler *et al.* [PHENIX Collaboration], arXiv:nucl-ex/0510047.
- [25] J. Bielcik [STAR Collaboration], arXiv:nucl-ex/0511005.
- [26] S. S. Adler *et al.* [PHENIX Collaboration], Phys. Rev. C **72**, 024901 (2005) [arXiv:nucl-ex/0502009].
- [27] D. Molnar and M. Gyulassy, Nucl. Phys. A **697**, 495 (2002) [Erratum-ibid. A **703**, 893 (2002)] [arXiv:nucl-th/0104073].
- [28] R. Baier, Y. L. Dokshitzer, A. H. Mueller, S. Peigne and D. Schiff, Nucl. Phys. B **483**, 291 (1997)
- [29] M. Gyulassy, P. Levai and I. Vitev, Phys. Rev. Lett. **85**, 5535 (2000)